

Co-localization of iron binding on silica with p62/sequestosome1 (SQSTM1) in lung granulomas of mice with acute silicosis

Yasuo Shimizu,^{1,2,3,*} Kunio Dobashi,⁴ Hiroyuki Nagase,⁵ Ken Ohta,⁶ Takaaki Sano,⁷ Shinichi Matsuzaki,³ Yoshiki Ishii,¹ Takahiro Satoh,⁸ Masashi Koka,⁸ Akihito Yokoyama,⁸ Takeru Ohkubo,⁸ Yasuyuki Ishii⁸ and Tomihiro Kamiya⁸

¹Department of Pulmonary Medicine and Clinical Immunology, Dokkyo Medical University School of Medicine, 880 Kitakobayashi, Mibu-machi, Tochigi 321-0293, Japan

²Department of Respiratory Medicine, Maebashi Red Cross Hospital, 3-21-36 Asahi-cho, Maebashi-shi, Tochigi 371-0014, Japan

³Department of Medicine and Molecular Science and ⁷Department of Diagnostic Pathology, Gunma University Graduate School of Medicine, 3-39-15 Showa-machi, Maebashi-shi, Gunma 371-8511, Japan

⁴Gunma University School of Health Sciences, 3-39-22 Showa-machi, Maebashi-shi, Gunma 371-8514, Japan

⁵Division of Respiratory Medicine and Allergology, Department of Medicine, Teikyo University School of Medicine, 2-11-1 Kaga, Itabashi-ku, Tokyo 173-8605, Japan

⁶Department of Respiratory Diseases, National Hospital Organization Tokyo National Hospital, Tokyo, 3-1-1 Takeoka, Kiyose-shi, Tokyo 204-8585, Japan

⁸Japan Atomic Energy Agency, Takasaki Advanced Radiation Research Institute, 1233 Watanuki-machi, Takasaki-shi, Gunma 370-1292, Japan

(Received 18 March, 2014; Accepted 2 September, 2014; Published online 28 November, 2014)

The cellular mechanisms involved in the development of silicosis have not been fully elucidated. This study aimed to examine influence of silica-induced lung injury on autophagy. Suspensions of crystalline silica particles were administered transnasally to C57BL/6j mice. Immunohistochemical examination for Fas and p62 protein expression was performed using lung tissue specimens. Two-dimensional and quantitative analysis of silica deposits in the lungs were performed *in situ* using lung tissue sections by an in-air microparticle induced X-ray emission (in-air micro-PIXE) analysis system, which was based on irradiation of specimens with a proton ion microbeam. Quantitative analysis showed a significant increase of iron levels on silica particles (assessed as the ratio of Fe relative to Si) on day 56 compared with day 7 ($p < 0.05$). Fas and p62 were expressed by histiocytes in granulomas on day 7, and the expressions persisted for day 56. Fas- and p62-expressing histiocytes were co-localized in granulomas with silica particles that showed an increase of iron levels on silica particles in mouse lungs. Iron complexed with silica induces apoptosis, and may lead to dysregulations of autophagy in histiocytes of granulomas, and these mechanisms may contribute to granuloma development and progression in silicosis.

Key Words: silicosis, apoptosis, autophagy, Fas, p62

Occupational and environmental exposure to silica leads to the development of silicosis.⁽¹⁾ The cellular mechanisms involved in silicosis have been investigated, and T cells and macrophages have been proven to be key participants in its initiation and progression.^(2–4) Granulomas develop in lungs with silicosis, and apoptosis has been demonstrated to be a pathway with a role in their development. Proapoptotic Fas protein and Fas ligand (FasL) are expressed by T cells and macrophages in animal models of silicosis and in patients with silicosis.^(5,6) In experimental model, the methodological difference of acute and chronic is that acute silicosis is induced by high dose silica instillation to trachea, but chronic silicosis is induced by low dose silica exposure using an aerosol chamber.⁽⁷⁾ Acute silica exposures induce granulomatous changes with loose aggregate of activated foamy histiocytes and lymphocytes, however chronic silica exposures induce well organized nodular structures consisting of epitheloid macrophages and multinucleated giant cells.⁽⁸⁾ In a mouse model

of acute silicosis, apoptosis has been proved to be important for granuloma development.⁽⁵⁾ On the other hand, in chronic silicosis model rats, apoptosis was less important during the late stage of granuloma development.⁽⁸⁾ In a murine model of acute silicosis, Fas- and FasL-expressing cells located in granulomas were almost macrophages positive for F4/80⁺. Small number of Fas- and FasL-expressing cells were lymphocytes negative for F4/80⁺.⁽⁵⁾ Macrophages phagocytose silica, and regulate the inflammatory production of cytokines such as interleukin-4 (IL-4), tumor necrosis factor- α (TNF- α), and interleukin-10 (IL-10). These cytokines have been proposed to play a role in fibrosis and granuloma formation.^(9–12)

Oxidative stress play a role in silica-induced lung injury, and iron complexed with silica (ICS) generates reactive oxygen species (ROS), with increased amounts of iron enhancing ROS production. Fenton reaction defined as $\text{Fe}^{2+} + \text{H}_2\text{O}_2$ goes $\text{Fe}^{3+} + \cdot\text{OH} + \text{OH}^-$ has been a proposed mechanism for silicate-induced ROS production.⁽¹³⁾ Silica dust obtained from the lungs of rats that received intratracheal instillation of silica had iron complexes on its surface, accompanied by elevation of ROS as shown by bronchial lavage.^(14–17) In rats, high amounts iron with silica produce more ROS *in vitro* than low amounts of iron with silica.⁽¹³⁾ An iron chelator diminished ROS production by THP-1 macrophages after silica exposure, and had the same effect in an *in vivo* rat silicosis model.^(18,19) The proposed mechanism of surface modification of inhaled silica involves the accumulation of ferritin and lactoferrin, as well as phospholipids and surfactant.^(20–22) Another potential source of iron that can complex with silica is the non-protein bound cellular iron pool associated with various low molecular weight compounds such as ATP, ADP, GTP, citrate, and free amino acids.⁽²³⁾

Autophagy is a regulated cellular pathway that is involved in the turnover of organelles and proteins by lysosomal-dependent processing.⁽²⁴⁾ Autophagy also acts as a survival mechanism under conditions of stress, maintaining cellular integrity by regenerating metabolic precursors and clearing subcellular debris.^(25–27) Triggers for the initiation of autophagy are stressors such as starvation or oxidative stress. Extrinsic particles can induce

*To whom correspondence should be addressed.
E-mail: yasuo-s@dokkyomed.ac.jp

autophagy via stress based on ROS production.^(28,29) Autophagy has been investigated in chronic obstructive pulmonary disease (COPD), pulmonary arterial hypertension, cystic fibrosis, lymph-angiomas, idiopathic pulmonary fibrosis (IPF), and acute hyperoxic lung injury,⁽³⁰⁾ however there have been no reports about it in silicosis. Inhibition of autophagy is correlated with an increase of p62, so analysis of p62 can assist in assessing the impairment of autophagy.⁽³¹⁾

In-air microparticle induced X-ray emission (in-air micro-PIXE) analysis is a method of performing elemental analysis by irradiation of the test material with a 3 MeV proton ion micro-beam. Irradiated samples yield specific X-ray patterns for various elements, and based on these patterns and their strength, an in-air micro-PIXE analysis system can visualize the spatial distribution and quantities of substances at a resolution of 1 μm .^(32,33) This system had been employed to investigate the association between the accumulation of particles in lung tissue and various pulmonary diseases, such as asbestosis, IPF, cryptogenic organizing pneumonia, interstitial pneumonia, and secondary pulmonary alveolar proteinosis.⁽³⁴⁾ Elemental analysis is also one of the methods for assessing particle deposition in tissues.

In this study, we employed in-air micro-PIXE analysis system to confirm the relation between silica deposition and expression of proteins related to apoptosis (Fas) and autophagy (p62) in granulomas by showing the co-localization of these proteins with silica particles. The spatial distribution of silica and iron, and quantitative analysis of iron on silica particles were also assessed by *in situ* analysis of lung tissue sections.

Materials and Methods

Animals. Pathogen-free C57BL/6j mice from Japan SLC (Shizuoka, Japan) were used for these experiments as described previously.⁽³⁵⁾ All animals were 6 to 8-week-old males and were maintained under standard conditions with free access to water and rodent laboratory food at the Division of Animal Research in the Teikyo University.

Instillation of silica. Acute lung injury was created by intranasal instillation of crystalline silica particles as described previously.^(2,35) Silica particles were obtained from Japan Association for Working Environment Measurement (Tokyo, Japan), and were suspended in saline at 200 mg/ml and ultrasonicated prior to use. The 40 μl of suspension was administered intranasally twice to each mouse (a total 16 mg/body) under anesthesia on day 0. As a control, PBS was administered intranasally in a similar manner. Mice were sacrificed under anesthesia with either on day 7 or day 56. The lungs were fixed in 10% formalin at a constant pressure (10 cm H_2O) overnight. Then the lungs were removed surgically for use in histological examination and elemental analysis. This study was approved by the Institutional Animal Care Committee of Teikyo University and Gunma University.

Immunohistochemical examination. Paraffin-embedded murine lung tissue specimens were cut into sections 4 μm thick and hematoxylin–eosin (HE) staining was performed as described previously.⁽³⁶⁾ For immunohistochemical staining, an anti-Fas rabbit polyclonal antibody (Calbiochem, Novabiochem, Boston, MA) and an anti-p62/sequestome (SQSTM1) rabbit polyclonal antibody (abcam, Cambridge UK) were used as the primary antibodies. The secondary antibody for Fas or p62 and a Simple Stain Mouse MAX PO (R) system (universal immunoperoxidase polymer for mouse tissue sections) were also used. Sections were examined under an Olympus BX53 microscope (Olympus, Tokyo, Japan), and a polarizing filter was used to detect silica particles in the immunostained sections.

In-air micro-PIXE analysis of silica in lung tissue sections. Serial paraffin-embedded murine lung tissue specimens used for immunohistochemistry were cut into sections 5 μm thick. Each section was dried, placed onto 5 μm polycarbonate film, and fixed

in the sample folder. Then elemental analysis was performed and deposition of silica particles in lung tissue was analysed *in situ* as reported previously.⁽³⁷⁾ Proton ion microbeam irradiation was done at the TIARA facility of the Japan Atomic Energy Agency (JAEA, Takasaki, Japan), and in-air micro-PIXE analysis was performed. Calculation of the relative quantity of each element was also performed as described previously.⁽³⁷⁾

The quantities of element A and element B were compared as follows:

$$\frac{m_B}{m_A} = \frac{Y_B M_B \text{eff}_A \sigma_A}{Y_A M_A \text{eff}_B \sigma_B}$$

where Y is the net count of the elements, M is the atomic weight of the element (amu), m is the quantity of the element in grams (g), eff is the detection efficiency for the element, and σ is the cross-sectional area of the specific X-ray peak for the element.

The ion microbeam was focused on areas ranging from 980 $\mu\text{m} \times 980 \mu\text{m}$ to 50 $\mu\text{m} \times 50 \mu\text{m}$, so the peaks of elements and two-dimensional elemental maps were obtained. The background lung tissue specimen is not homogenous and sulphur (S) is regarded as being representative of the total cell count and background tissue.⁽³⁸⁾ Therefore, to normalize Silica (Si) X-ray data for the background lung tissue, the Si/S ratio was calculated. Phosphorus (P) reflects cell morphology, because P is a major component of cell membranes. Therefore, mapping of P was used to identify cells in two-dimensional analysis.⁽³⁹⁾

In the first analysis, to confirm the amount of silica particles in the lung tissue sections, the Si/S ratio was assessed in 980 $\mu\text{m} \times 980 \mu\text{m}$ of large areas. Five lung tissue specimens from mice were observed in each group ($n = 5$). In the second analysis, to investigate iron (Fe) levels on Si particles in lung tissue sections, the ion microbeam was focused on silica particles located in granulomatous lesions. The Fe to Si (Fe/Si) ratio was assessed in 50 $\mu\text{m} \times 50 \mu\text{m}$ small areas on day 7 and day 56. Four silica particles deposited in granulomas in a lung tissue section were examined in a silica treated mouse. Therefore, a total of 20 silica particles of each mouse lung tissue section were examined on day 7 and day 56. Gating method to silica particles by in-air micro-PIXE analysis were described as previously.⁽³⁷⁾

Statistical analysis. Differences between groups were assessed by Student's *t* test. Results are presented as the mean \pm SD. Statistical analyses were performed using GraphPad Prism software and significance was accepted at $*p < 0.05$.

Results

Instillation of crystalline silica particles into mice caused interstitial pneumonitis with thickening of the alveolar septae and formation of granulomas, as demonstrated previously.⁽²⁾ These lesions appeared by day 7, and were also seen on day 56. In contrast, such lesions were not observed in control mice on day 7 or day 56 (Fig. 1a–f).

In the first elemental analysis, which was performed to quantify the content of crystalline silica particles in lung tissue, the ion microbeam was focused on large areas (980 $\mu\text{m} \times 980 \mu\text{m}$) of the tissue sections. On both day 7 and day 56, lung tissue sections from mice treated with silica particles showed higher Si peaks than sections from control mice (Fig. 2a–d). The ratio of Si to S (Si/S ratio) on day 7 and day 56 was calculated by the in-air micro-PIXE analysis system. The mean Si/S ratio was 4.3 ± 5.1 in silicosis mice and 0.5 ± 0.1 in control mice on day 7 ($n = 5$). On day 56, the mean Si/S ratio was 2.2 ± 0.9 in silicosis mice and 0.5 ± 0.1 in control mice ($n = 5$). Statistical analysis showed that Si content was significantly higher in lung tissue sections from silicosis mice than control mice on both day 7 and day 56 (Fig. 2e and f).

In the second elemental analysis, which was done to examine

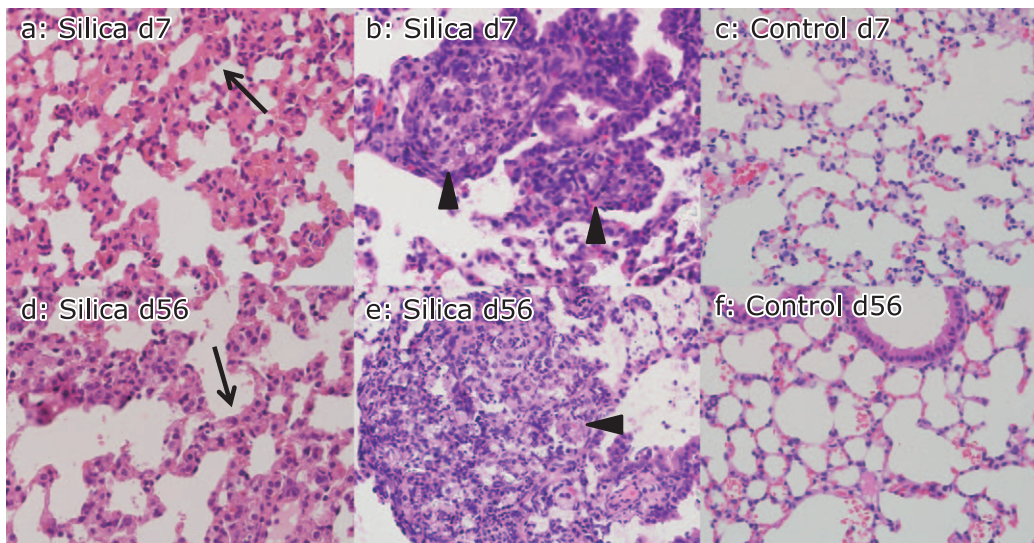


Fig. 1. Interstitial pneumonitis and granulomas induced by instillation of crystalline silica particles. Instillation of crystalline silica particles caused interstitial pneumonitis with thickening of the alveolar septae (arrow) and formation of granulomas (arrowhead) as shown by hematoxylin–eosin (HE) staining. Interstitial pneumonitis (a) and granuloma (b) were observed in silica-treated mice (silicosis mice) on day 7, while instillation of PBS (control mice) did not cause such changes on day 7 (c). Interstitial pneumonitis (d) and granulomas (e) were observed in silica-treated mice (silicosis mice) on day 56. Control mice did not show inflammatory changes on day 56 (f). Silica-induced inflammatory changes of the lungs appeared at an early stage (day 7) and also persisted to day 56 (magnification: 400 \times).

the co-localization of iron and silica in the lungs, or the changes of iron (Fe) levels in a silica particle, the ion microbeam was focused on smaller areas (50 $\mu\text{m} \times 50 \mu\text{m}$) of silica particles in granulomatous lesions on day 7 and day 56. Peaks of Si (red), Fe (blue) and P (light blue) were indicated in day 7 (Fig. 3a) and day 56 (Fig. 3b). P mapping was used to identify the location of cells around the silica particles. Both peaks of Si and Fe were high in day 7 (Fig. 3a) and day 56 (Fig. 3b). Then analysis was done by gating on silica particles using the in-air micro-PIXE analysis system, as previously.⁽³⁷⁾ When two-color elemental maps that displayed the spatial distribution of Si (red) and Fe (green) in lung tissue were overlaid using the in-air micro-PIXE system, ICS was shown as yellow (the red of Si mixed with the green of Fe) in the lung tissue of from silicosis mice on day 7 (Fig. 3c) and day 56 (Fig. 3d). The size and number of accumulated Fe atoms on the surface of silica particles were increased on day 56 compared with day 7. Fe/Si ratio was calculated by in-air micro-PIXE analysis system. The mean Fe/Si ratio was 0.0021 ± 0.0028 on day 7 and 0.0067 ± 0.0071 on day 56 ($n = 20$). Statistical analysis showed that the Fe/Si ratio was significantly higher on day 56 than on day 7 (Fig. 3e). There were fine green-outlined shapes, which were considered histiocytes, around silica particles on day 56 (Fig. 3d). To confirm the increased intracellular iron levels, Fe/P ratio was calculated. Sulphur (S) is regarded as being representative of the total cell count and background tissue and P was used to assess cell morphology. P is well reflected cell morphology, but not well reflects other components of lung tissue. On day 7, elemental map showed that silica particles (Fig. 3f) were surrounded with cells, which were identified by P (Fig. 3g). On day 56, elemental map showed that silica particles (Fig. 3h) were surrounded with cells, which were identified by P (Fig. 3i). Both day 7 and day 56 of silica particles were surrounded with cells. When identification of cells by P mapping by in air micro-PIXE analysis, cells located in around crystalline silica particles were found to be high Fe (green) content on day 56 compared to day 7 (Fig. 3c and d). To calculate the intracellular Fe content, the cells were gated on two dimensional map, and the calculation was done by in air microPIXE system as previously.⁽³⁷⁾ The mean P/S (cell/background tissue) ratio was not statistically different between day 7

(1.47 ± 0.5) and day 56 (1.41 ± 0.3) on cells, but the mean Fe/P (intracellular Fe/cell) ratio was statistically higher on day 56 (0.013 ± 0.005) compared to day 7 (0.010 ± 0.012) ($p = 0.0018$, graphs of P/S and Fe/P were not shown).

Iron deposited in tissues has been reported to cause marked oxidative stress. To explore the possible roles of ICS in lung tissue damage, the expression of proteins related to apoptosis and autophagy was examined in lung tissue sections by immunohistochemical analysis. On day 7, proapoptotic Fas protein was expressed by histiocytes accumulating in granulomatous lesions of the peripheral bronchioles adjacent to the alveoli, as well as by type II pneumocytes, histiocytes in the alveolar septae, and bronchial epithelial cells in silicosis mice (Fig. 4a–c). In contrast, Fas was not expressed in control mice on day 7 (Fig. 4d–f). An increase of p62 is correlated with inhibition of autophagy. On day 7, p62 was expressed by histiocytes accumulating in granulomatous lesions of the peripheral bronchioles adjacent to the alveoli, but it was not expressed by type II pneumocytes, histiocytes in the alveolar septae, or bronchial epithelial cells in silicosis mice (Fig. 5a–c). In addition, p62 was not expressed in control mice on day 7 (Fig. 5d–f).

On day 56, there was increased Fas expression by histiocytes in the granulomatous lesions of peripheral bronchioles adjacent to the alveoli, as well as by type II pneumocytes, histiocytes in the alveolar septae, and bronchial epithelial cells of silicosis mice (Fig. 6a–c). Co-localization of silica particles and these Fas-expressing cells was confirmed by polarizing microscopy (Fig. 6d). There were Fas positive histiocytes phagocytosed silica particles (Fig. 6e) or accumulated around the silica particles (Fig. 6f). In contrast, Fas was not expressed in control mice on day 56 (Fig. 6g and h). In silicosis mice, polarizing microscopic analysis showed increased Fas expression by type II pneumocytes and bronchial epithelial cells corresponding to the sites of heavy silica particle deposition rather than the sites of low silica particle deposition (Fig. 7a and b).

On day 56, p62 expression by histiocytes of granulomatous lesions in the peripheral bronchioles adjacent to the alveoli (Fig. 8a). p62 was not expressed in bronchial epithelial cells or type II pneumocytes (Fig. 8b and c). Co-localization of crystalline

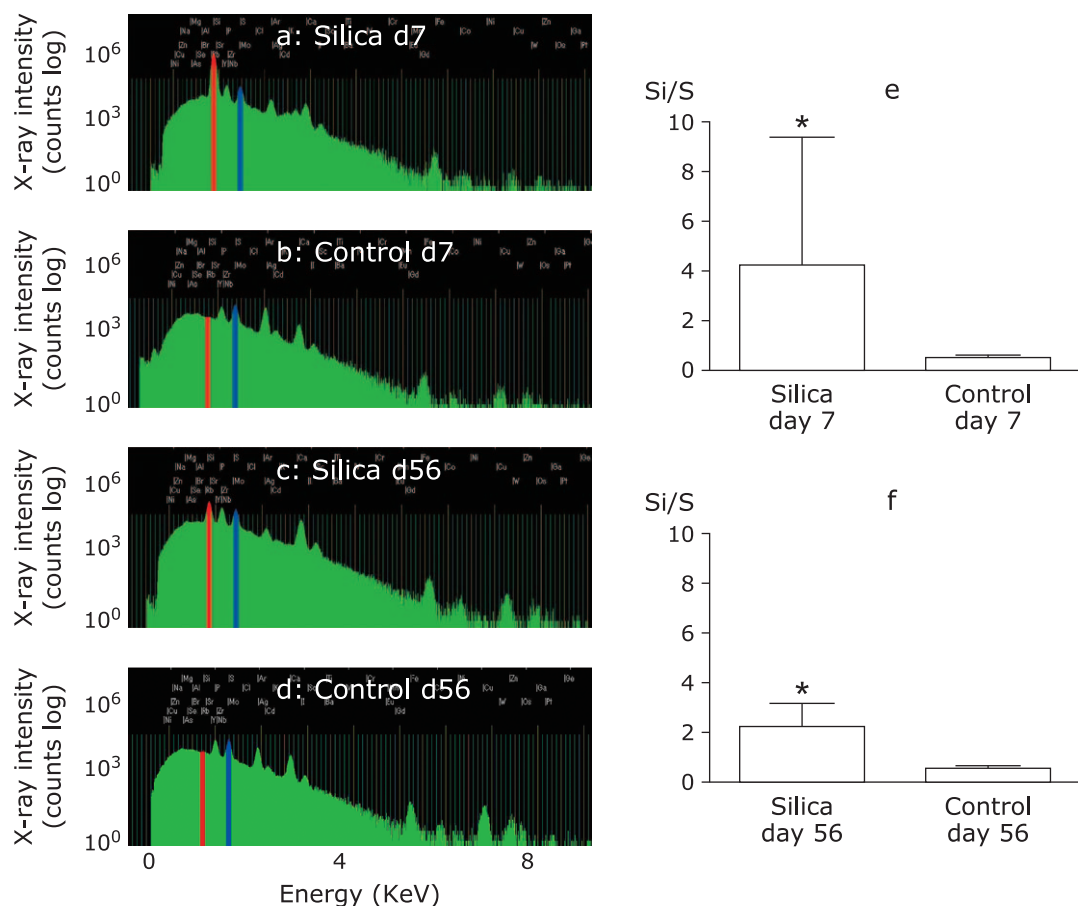


Fig. 2. Confirmation of crystalline silica deposition in lung by the analysis on large area (980 $\mu\text{m} \times 980 \mu\text{m}$) of lung tissue section. Peaks of Si in silicosis and control mice were analysed by in-air micro-PIXE analysis. Analysis was done on lung tissue sections from mice. Peaks of Si (red) were higher in silicosis mice (a) than control mice (b) on day 7. Peaks of Si (red) were also higher in silicosis mice (c) than control mice (d) on day 56. The background lung tissue specimen is not homogenous and sulphur (S) is regarded as being representative of the total cell count and background tissue. Therefore, to normalize Si X-ray data for the background lung tissue, the Si/S ratio was calculated. The peaks of S were indicated as blue. Quantitative analysis of lung tissue sections showed that the Si/S ratio was significantly higher in silicosis mice than in control mice on day 7 (e) and day 56 (f) (* $p < 0.05$).

silica particles and p62-expressing cells was confirmed by polarizing microscopy (Fig. 8d). There were p62 positive histiocytes phagocytosed silica particles (Fig. 8e) or accumulated around the silica particles (Fig. 8f). In contrast, p62 was not expressed in control mice on day 56 (Fig. 8g and h).

Discussion

It is known that apoptosis is associated with silica-induced acute lung injury.^(1,5,40) In a murine silicosis model, the concentration of TNF- α in bronchoalveolar lavage fluid (BALF) was found to be increased, and proapoptotic Fas and FasL mediated the apoptosis of T lymphocytes and alveolar macrophages.^(5,40) The present study showed prominent accumulation of Fas-expressing histiocytes in pulmonary granulomas. Fas expression was observed at an early stage (day 7) in these sites, and the expressions persisted to day 56, in accordance with previous reports.^(5,40) Fas- and FasL-expressing cells located in granulomas were almost macrophages positive for F4/80⁺. Small number of Fas- and FasL-expressing cells were lymphocytes negative for F4/80⁺.⁽⁵⁾ Based on these reports, the histiocytes seen in granulomas in the present study were possibly also macrophages. In an analysis of BALF obtained from patients with silicosis, Fas/FasL pathway-mediated apoptosis of alveolar macrophages was demonstrated to be

involved in silicosis.⁽⁴¹⁾ Thus, Fas-mediated apoptosis of macrophages has been proven to make a contribution to silica-induced lung injury.

In a rat model of experimental chronic silicosis, most silica particles were cleared from the lungs, but smaller number of silica particles phagocytosed by macrophages were retained in the lungs.⁽⁸⁾ In an acute silicosis animal model, however, there has been no report about the comparison in lung content of silica in the early (day 7) and late stages (day 56). The present study employed in-air micro-PIXE analysis to assess silica particles in lung tissue sections, and revealed a decrease of silica particles to half the amount on day 56 compared with day 7. As the seen in chronic silicosis models, silica particles in acute model induced the development of granulomas in the lung parenchyma in a time-dependent manner, as we and others have previously demonstrated on the basis of histological scores in acute silicosis models.^(2,42) This also suggested that silica particles can be removed from the lungs after acute exposure by expectoration, but residual particles contribute to promote granuloma formation.

Although Fas-mediated apoptosis makes a proven contribution to silica-induced lung injury, to explore other mechanisms underlying granuloma development in the acute silicosis model, we investigated the role of autophagy. Microtubule-associated protein light chain (LC3) is one of the autophagy-related (ATG)

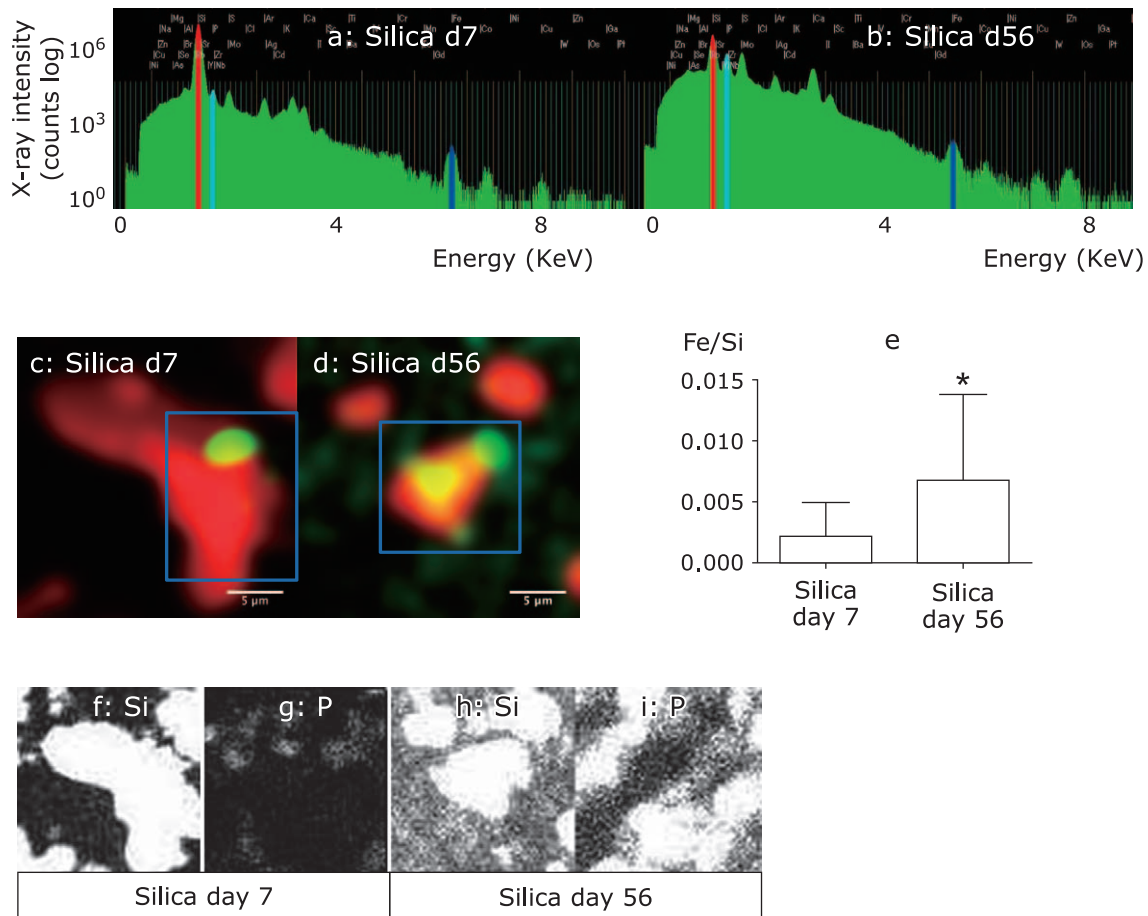


Fig. 3. Increase in Fe level in a silica particle located in the granulomas and histiocytes around the silica particles of silicosis mice after two month from silica instillation. Ion-microbeam was irradiated to the silica particles located in granuloma ($50 \mu\text{m} \times 50 \mu\text{m}$). Peaks of Si (red), Fe (blue) and P (light blue) were indicated in day 7 (a) and day 56 (b) of silicosis mice lung tissue sections. P mapping was used to identify the locations of cells around the silica particles. Both peaks of Si and Fe were high in day 7 (a) and day 56 (b). Two-color elemental maps that displayed the spatial distribution of Si (red) and Fe (green) in silica were overlaid using the in-air micro-PIXE analysis system. ICS is shown as yellow (red of Si mixed with green of Fe) on day 7 (c) and day 56 (d) in silicosis mice. The size and number of Fe on the surface of crystalline silica particles were increased in lung tissue sections from silicosis mice on day 56 compared to day 7. Scale bar = $5 \mu\text{m}$. Quantitative analysis of Fe focused on silica particles showed that the Fe to Si (Fe/Si) ratio was significantly higher on day 56 than day 7 (e) ($*p < 0.05$). On day 56, weak green-outlined cells, which were inflammatory cells identified by P mapping, appeared around the silica particles (d). To show the increased iron levels in cells around silica particles on day 56, elemental map analysis was done on Si and P. On day 7, elemental map showed that silica particles (f) were surrounded with cells, which were identified by P (g). On day 56, elemental map showed that silica particles (h) were surrounded with cells, which were identified by P (i). Both day 7 and day 56 of silica were surrounded with cells. However on day 56, weak green-outlined cells, which were inflammatory cells identified by P mapping, appeared around the silica particles (d), but there were no such green-outlined cells around the silica particles on day 7 (c). Two-color elemental maps that displayed the spatial distribution of Si (red) and Fe (green) in figure c and d, as above described. Therefore, on day 56, these green-outlined cells contained increase in intracellular iron compared to day 7. The statistical results for quantitative analysis of Fe/P were described in the results section.

proteins that is located on autophagosomes.⁽²⁴⁾ The protein p62 binds ubiquitin and LC3, and is a selective substrate of autophagy that regulates the formation of protein aggregates.⁽⁴³⁾

In the present study, elevated expression of p62 was mostly observed in the histiocytes of granulomas. The expression was observed in the early stage on day 7 and persisted to day 56 during the present study. As mentioned above, the cells in granulomas were almost all macrophages positive for F4/80⁺,⁽⁵⁾ and cells expressing p62 in the granulomas were considered to be macrophages. The increase of p62 expression in macrophages from the granulomas indicated that impairment of autophagy occurred from an early stage (day 7) in these cells and continued to day 56.

There have been many reports that surface modification of iron on silica enhances lung injury with elevation of ROS. Triggers for the initiation of autophagy are stressors such as starvation or oxidative stress.^(28,29) Extrinsic particles can induce autophagy via

stress based on ROS production. Phospholipid is a component of alveolar surfactant, and exposure of oxidative stress is associated with an accumulation of surfactant in alveoli.⁽⁴⁴⁾ We did not directly showed the elevation of oxidative stress markers in present study, however we previously reported the elevation of phospholipid in BAL after silica instillation to lung.⁽²⁾ A previous report showed that phospholipid concentration after silica instillation to lung was associated with complexed Fe³⁺ on silica surface.⁽¹⁵⁾

The proposed mechanism of increase in iron (Fe) levels in a silica particles in lung were that inhaled silica binds the accumulated ferritin and lactoferrin, as well as phospholipids and surfactant in lung.⁽²⁰⁻²²⁾ Another potential source of iron that can complex with silica is the non-protein bound cellular iron pool associated with various low molecular weight compounds such as ATP, ADP, GTP, citrate, and free amino acids.⁽²³⁾ Similar changes had been reported in surface modification of asbestos.⁽⁴⁵⁾

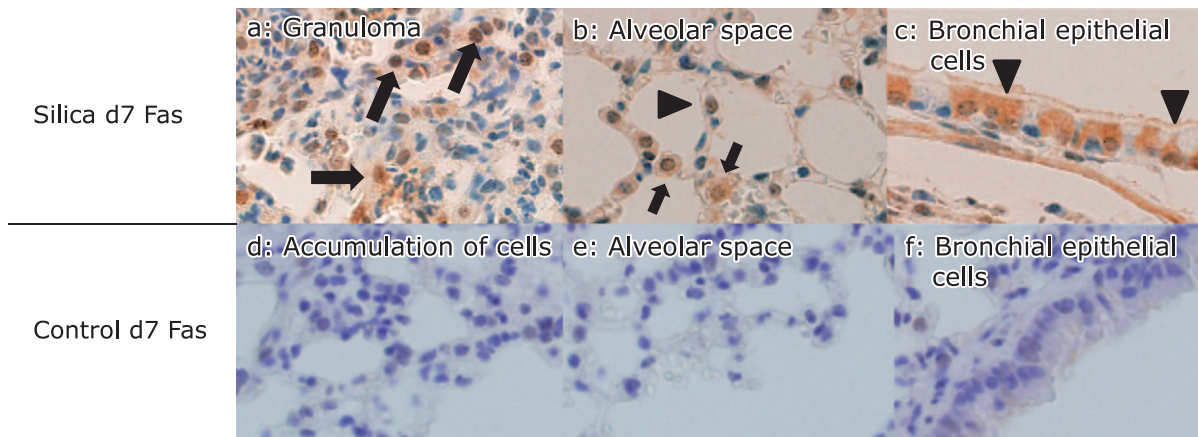


Fig. 4. Fas expression in lung tissue sections from silicosis mice on day 7. Fas was expressed by histiocytes in granulomatous lesions of the peripheral bronchioles adjacent to the alveoli (a, arrow), and also by type II pneumocytes (b, arrowhead), histiocytes in alveolar septae (b, arrow), and bronchial epithelial cells (c, arrowhead) on day 7 in silicosis mice. In contrast, Fas was not expressed in these cells of control mice on day 7 (d–f). There were no granulomas in control lung, and accumulated cells observed in lung tissue specimens also did not express Fas (d)(magnification: 400 \times).

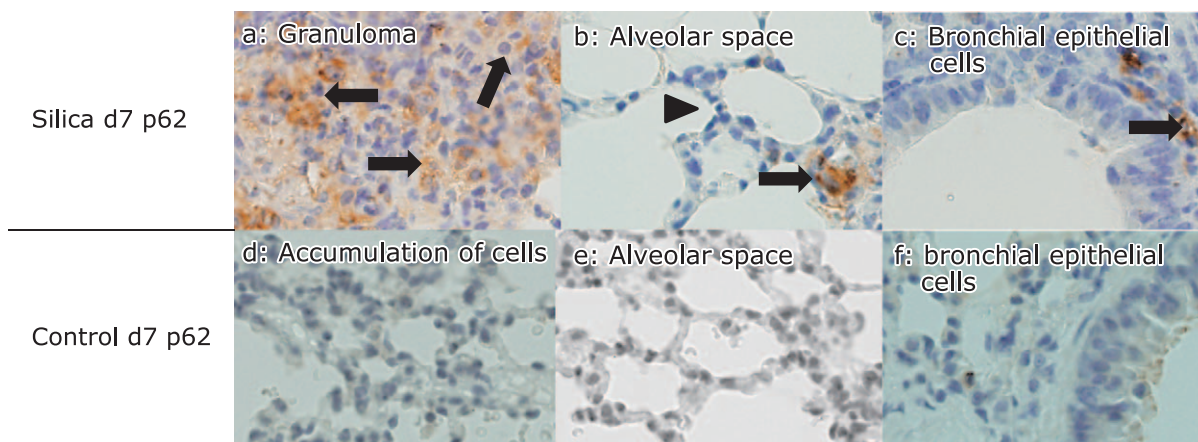


Fig. 5. p62 expression in lung tissue sections from silicosis mice on day 7. p62 was expressed by histiocytes in granulomatous lesions of the peripheral bronchioles adjacent to the alveoli (a, arrows). p62 was not expressed by type II pneumocytes (b, arrowhead). Histiocytes located in interstitium were seen (b, arrow). Bronchial epithelial cells did not express p62, but several interstitial histiocytes expressed p62 (c, arrow). p62 was not expressed in lung tissues from control mice on day 7 (d–f). There were no granulomas in control lung. Accumulated cells observed in lung tissue specimens also did not express p62 (d) (magnification: 400 \times).

Intracellular iron levels evaluated by Fe/P ratio were elevated on day 56. Increase in Fe levels of cells have been reported in silica particle exposure to cells.⁽⁴⁶⁾ Exposure of both silica and ferric acid enhanced the increase in intracellular non-heme iron and ferritin compared to only silica exposure. Increase of intracellular Fe levels was protective mechanisms of cells against oxidative stress associated with particle matter exposure.⁽⁴⁶⁾ The reason of elevation of Fe/P ratio in cells on day 56 might reflect the protective mechanisms of cells against oxidative stress, which was caused by increase in iron levels on silica particles.

Since ICS produces ROS, which trigger autophagy, we employed in-air micro-PIXE analysis to investigate ICS in granulomas by *in situ* analysis of lung tissue sections. In air micro-PIXE analysis revealed an existence of ICS in the lung granulomas by both two-dimensional and quantitative analysis, and iron levels in silica particle was increased on day 56 compared with day 7. These findings suggested that increased ROS production might accompany the increase in iron levels of silica particle, leading to impairment of autophagy by macrophages in the

granulomas, and that impairment of autophagy might play a role in the development of granulomas associated with silicosis.

Impairment of autophagy along with an increase of p62 has already been documented in IPF and COPD. In IPF, p62 protein levels were increased in whole lung lysate, and impairment of autophagy due to TGF- β 1 production was involved in the mechanism of fibrogenesis.⁽⁴⁷⁾ Interestingly, peripheral blood macrophages from smokers show impairment of autophagy with increased expression of p62 protein.⁽⁴⁸⁾ Although impairment of autophagy along with increased expression of p62 protein has thus been demonstrated in IPF lung tissue and in the macrophages of cigarette smokers,^(47–49) the role of autophagy in silicosis has not been explored. Inhibition of autophagy is correlated with an increase of p62, so analysis of p62 can assist in assessing the impairment of autophagy.^(24,31)

The present study showed both Fas and p62 expressions in granulomas. There have been several reports about Fas and p62 crosstalk. p62 acts as a signaling adaptor in apoptosis and autophagy.^(50,51) When lung injury occurs, hyperoxia disrupts the

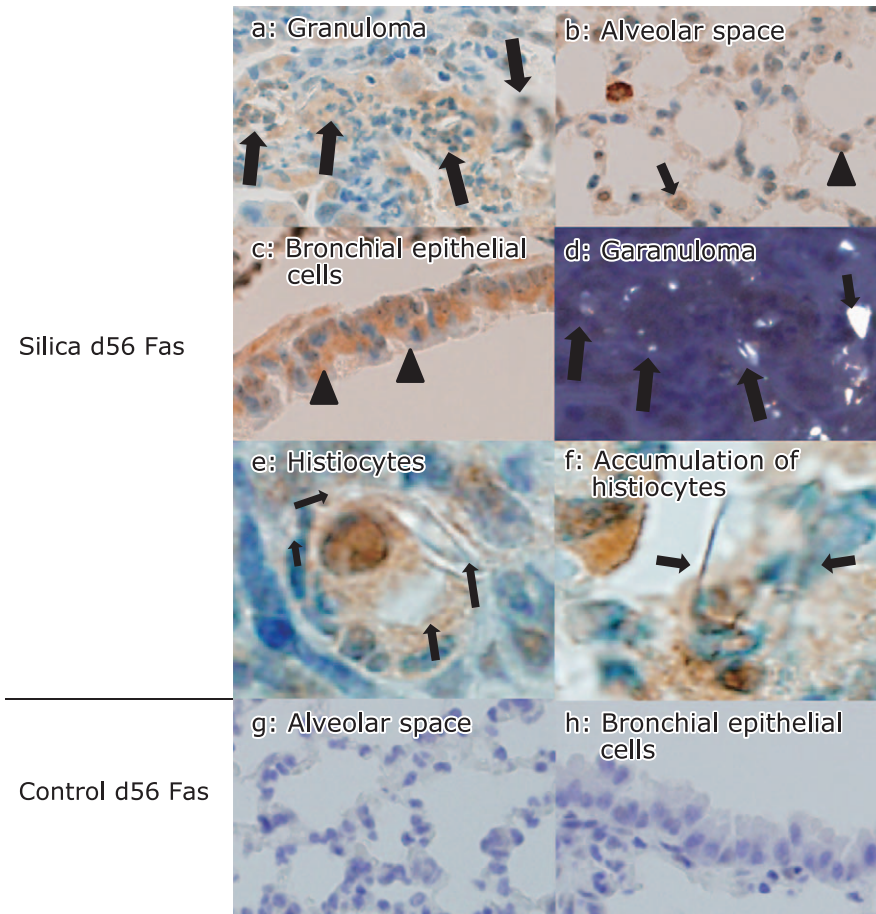


Fig. 6. Fas expression was persistent in lung tissue sections from silicosis mice on day 56. Fas was expressed by histiocytes in granulomatous lesions of the peripheral bronchioles adjacent to the alveoli (a, arrows), type II pneumocytes (b, arrowhead) and histiocytes in the alveolar septae (b, arrow), as well as by bronchial epithelial cells (c, arrowheads). Co-localization of crystalline silica particles and Fas-expressing cells in granulomas was confirmed by polarizing microscopy (polarized on figure a) (magnification: 400 \times). Silica particles were seen as white dots (d, arrows). There were Fas positive histiocytes phagocytosed silica particles (e) or accumulated around the silica particles (f). Arrows indicate silica particles (magnification: oil immersion, 1,000 \times). In control mice, Fas was not expressed in lung tissues on day 56 (g and h) (magnification: 400 \times).

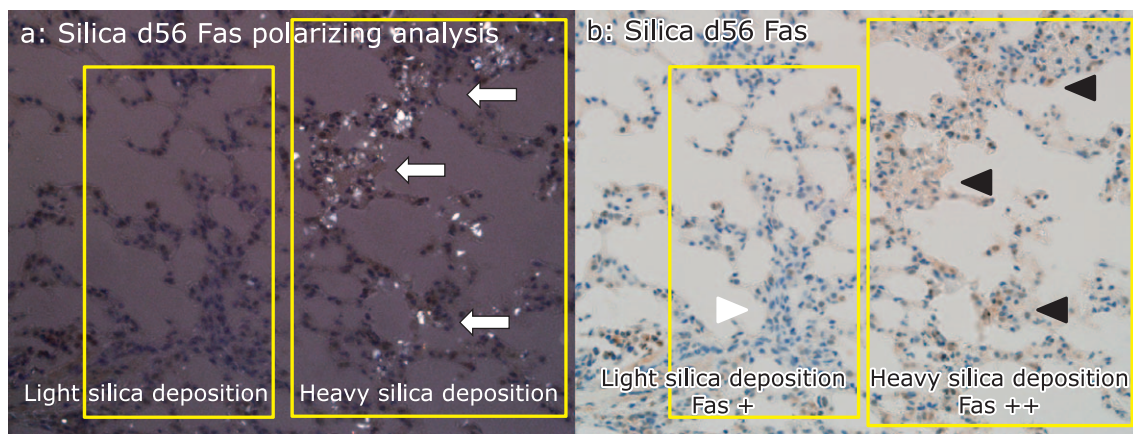


Fig. 7. Fas expression was higher at the sites of heavy silica particle deposition area compared to light deposition area in silicosis mice lung on day 56. Polarizing microscopic analysis indicates the heavy silica particle deposition and light silica deposition areas (a, yellow squares). In heavy silica particle deposition area, dense silica particles were seen as white dots (arrows). Fas expressions by histiocytes of peripheral bronchioles adjacent to the alveoli were higher at the sites of heavy silica particle deposition (b, black arrowheads) than at the sites of light particle deposition (b, white arrowhead). (magnification: 400 \times).

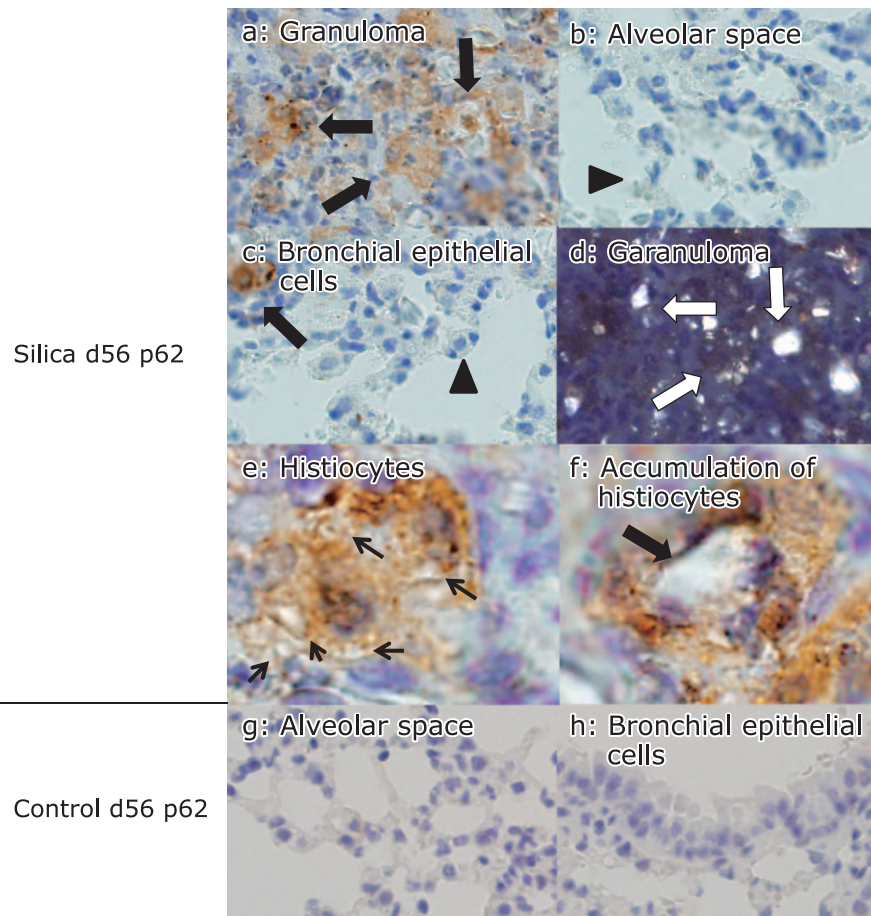


Fig. 8. p62 expression was persistent in lung tissue sections from silicosis mice on day 56. p62 was expressed by histiocytes in granulomatous lesions of the peripheral bronchioles adjacent to the alveoli (a, arrows), however p62 was not expressed by type II pneumocytes (b, arrowhead) bronchial epithelial cells (c, arrowhead). Histiocytes located in interstitium were seen (c, arrow). Co-localization of silica particles and p62-expressing cells was confirmed by polarizing microscopy in granuloma (polarized on figure a). Silica particles appeared as white dots (d, arrows) (magnification: 400 \times). There were p62 positive histiocytes phagocytosed silica particles (e) or accumulated around the silica particles (f). Arrows indicate silica particles (magnification: oil immersion, 1,000 \times). In contrast, p62 was not expressed in lung tissues from control mice (g and h) (magnification: 400 \times).

p62-Fas complex, and p62 regulates apoptosis after hyperoxia. LC3b is an autophagy-related ubiquitin-like modifier, and it forms a complex with p62 to regulate cytoprotection of alveolar epithelial cells after hyperoxia.⁽⁵²⁾ These findings suggest that apoptosis can occur at the same time as autophagy,⁽²⁴⁾ so synchronous Fas and p62 expression in the macrophages of silicosis granulomas indicated crosstalk between these molecules in the present study. Instillation of crystalline silica particles led to accumulation of particles complexed with iron in granulomas. The amount of iron associated with silica increased over time along with increased expression of Fas and p62. The accumulation of ICS may induce apoptosis and impairment of autophagy in macrophages by promoting ROS production, contributing to granuloma development in silicosis.

There are several limitations of this study. We investigated ICS for the purpose of assessing the mechanisms underlying ROS-mediated apoptosis and impairment of autophagy in a mouse model of acute silicosis. It was proven that an increase of ROS levels is dependent on the iron level, but whether p62 expression is affected by iron was not directly demonstrated. There have been a few reports of metals on autophagy. Brain iron accumulation and p62-positive glial inclusions are found in Huntington's disease.⁽⁵³⁾ Iron oxide nanoparticles induce ROS, leading to mitochondrial damage and autophagy in lung epithelial cancer cells.⁽⁵⁴⁾ SiO₂ nanoparticles induce less autophagy than copper oxide, while iron

oxide nanoparticles appeared to have no cytotoxic effect on A549 lung cancer cells.⁽⁵⁵⁾ Thus, whether p62 expression is affected by iron has not been established. The size of crystalline silica particles can influence the cellular response. Rat macrophages show a stronger apoptotic response to smaller silica particles than larger particles.⁽⁵⁶⁾ The crystalline silica particles used in the present study ranged from 2 μ m to 20 μ m as assessed by in-air micro-PIXE analysis, and these sizes were similar to those used in previous reports.^(16,57) Whether p62 expression can be affected by silica particle size has not been established. Furthermore, over expression of p62 is not necessary related to impairment of autophagy, and in some conditions, the expression is related to activation of autophagy.⁽⁵²⁾

Taken together, the present study showed co-localization of Fas and p62 expression in the macrophages of granulomas along with silica particles that displayed an increase of ICS in mice with acute silicosis. Investigation of whether different amounts and sizes of ICS have different effects on autophagy in silicosis will need to be done in the future.

Authors' Contributions

Y. Shimizu designed this study, immunostained the lung tissues and analysed immunostained samples, analysed the PIXE data, and wrote this manuscript. K. Dobashi irradiated the samples and

analysed immunostained samples, and gave useful suggestions about in-air micro-PIXE analysis. H. Nagase performed the animal experiments, and designed this study. K. Ohta established the animal experiments. T. Sano analysed the immunostained samples. Y. Ishii advised the pathogenesis of silicosis. S. Matsuzaki prepared the samples and irradiated the samples. T. Satoh analysed the data and irradiated the samples. M. Koka, A. Yokoyama, T. Ohkubo, Y. Ishii, and T. Kamiya irradiated the samples.

Acknowledgments

We thank H. Ito M.D., Maebashi Red Cross Hospital and F. Yokotsuka, Research Support Centre of Dokkyo University for facilitation of microscopic analysis. This work was supported by a grant (No. 24310067) from the Ministry of Education, Science and Culture, Japan.

Conflict of Interest

No potential conflicts of interest were disclosed.

References

- Hamilton RF Jr, Thakur SA, Holian A. Silica binding and toxicity in alveolar macrophages. *Free Radic Biol Med* 2008; **44**: 1246–1258.
- Suzuki N, Ohta K, Horiuchi T, et al. T lymphocytes and silica-induced pulmonary inflammation and fibrosis in mice. *Thorax* 1996; **51**: 1036–1042.
- Hubbard AK. Role for T lymphocytes in silica-induced pulmonary inflammation. *Lab Invest* 1989; **61**: 46–52.
- Beamer CA, Migliaccio CT, Jessop F, Trapkus M, Yuan D, Holian A. Innate immune processes are sufficient for driving silicosis in mice. *J Leukoc Biol* 2010; **88**: 547–557.
- Borges VM, Falcão H, Leite-Júnior JH, et al. Fas ligand triggers pulmonary silicosis. *J Exp Med* 2001; **194**: 155–164.
- Otsuki T, Hayashi H, Nishimura Y, et al. Dysregulation of autoimmunity caused by silica exposure and alteration of Fas-mediated apoptosis in T lymphocytes derived from silicosis patients. *Int J Immunopathol Pharmacol* 2011; **24**: 11S–16S.
- Langley RJ, Mishra NC, Peña-Philippides JC, Hutt JA, Sopori ML. Granuloma formation induced by low-dose chronic silica inhalation is associated with an anti-apoptotic response in Lewis rats. *J Toxicol Environ Health A* 2010; **73**: 669–683.
- Langley RJ, Kalra R, Mishra NC, et al. A biphasic response to silica: I. Immunostimulation is restricted to the early stage of silicosis in lewis rats. *Am J Respir Cell Mol Biol* 2004; **30**: 823–829.
- Gilberti RM, Joshi GN, Knecht DA. The phagocytosis of crystalline silica particles by macrophages. *Am J Respir Cell Mol Biol* 2008; **39**: 619–627.
- Arras M, Huaux F, Vink A, et al. Interleukin-9 reduces lung fibrosis and type 2 immune polarization induced by silica particles in a murine model. *Am J Respir Cell Mol Biol* 2001; **24**: 368–375.
- Liu H, Zhang H, Forman HJ. Silica induces macrophage cytokines through phosphatidylcholine-specific phospholipase C with hydrogen peroxide. *Am J Respir Cell Mol Biol* 2007; **36**: 594–599.
- Huaux F, Louahed J, Hudspeth B, et al. Role of interleukin-10 in the lung response to silica in mice. *Am J Respir Cell Mol Biol* 1998; **18**: 51–59.
- Castranova V, Vallyathan V, Ramsey DM, et al. Augmentation of pulmonary reactions to quartz inhalation by trace amounts of iron-containing particles. *Environ Health Perspect* 1997; **105**(Suppl 5): 1319–1324.
- Ghio AJ, Kennedy TP, Whorton AR, Crumbliss AL, Hatch GE, Hoidal JR. Role of surface complexed iron in oxidant generation and lung inflammation induced by silicates. *Am J Physiol* 1992; **263**: L511–L518.
- Ghio AJ, Hatch GE. Lavage phospholipid concentration after silica instillation in the rat is associated with complexed [Fe³⁺] on the dust surface. *Am J Respir Cell Mol Biol* 1993; **8**: 403–407.
- Ghio AJ, Jaskot RH, Hatch GE. Lung injury after silica instillation is associated with an accumulation of iron in rats. *Am J Physiol* 1994; **267**: L686–L692.
- Seal S, Krezoski S, Barr TL, Petering DH, Klinowski J, Evans PH. Surface chemistry and biological pathogenicity of silicates: an X-ray photoelectron spectroscopic study. *Proc Biol Sci* 1996; **263**: 943–951.
- Premasekharan G, Nguyen K, Contreras J, Ramon V, Leppert VJ, Forman HJ. Iron-mediated lipid peroxidation and lipid raft disruption in low-dose silica-induced macrophage cytokine production. *Free Radic Biol Med* 2011; **51**: 1184–1194.
- Ghio AJ, Kennedy TP, Crissman KM, Richards JH, Hatch GE. Depletion of iron and ascorbate in rodents diminishes lung injury after silica. *Exp Lung Res* 1998; **24**: 219–232.
- Rivers D, Wise ME, King EJ, Nagelschmidt G. Dust content, radiology, and pathology in simple pneumoconiosis of coalworkers. *Br J Ind Med* 1960; **17**: 87–108.
- Miles PR, Bowman L, Jones WG, Berry DS, Vallyathan V. Changes in alveolar lavage materials and lung microsomal xenobiotic metabolism following exposures to HCl-washed or unwashed crystalline silica. *Toxicol Appl Pharmacol* 1994; **129**: 235–242.
- Viviano CJ, Bakewell WE, Dixon D, Dethloff LA, Hook GE. Altered regulation of surfactant phospholipid and protein A during acute pulmonary inflammation. *Biochim Biophys Acta* 1995; **1259**: 235–244.
- Gutteridge JMC, Halliwell B. *Iron transport and storage*. Boca Raton FL: CRC Inc., 1990; 55–66.
- Mizumura K, Cloonan SM, Haspel JA, Choi AM. The emerging importance of autophagy in pulmonary diseases. *Chest* 2012; **142**: 1289–1299.
- Levine B, Kroemer G. Autophagy in the pathogenesis of disease. *Cell* 2008; **132**: 27–42.
- Mizushima N, Levine B, Cuervo AM, Klionsky DJ. Autophagy fights disease through cellular self-digestion. *Nature* 2008; **451**: 1069–1075.
- Ravikumar B, Moreau K, Jahreiss L, Puri C, Rubinsztein DC. Plasma membrane contributes to the formation of pre-autophagosomal structures. *Nat Cell Biol* 2010; **12**: 747–757.
- Lee J, Giordano S, Zhang J. Autophagy, mitochondria and oxidative stress: cross-talk and redox signalling. *Biochem J* 2012; **441**: 523–540.
- Choi AM, Ryter SW, Levine B. Autophagy in human health and disease. *N Engl J Med* 2013; **368**: 651–662.
- Patel AS, Morse D, Choi AM. Regulation and functional significance of autophagy in respiratory cell biology and disease. *Am J Respir Cell Mol Biol* 2013; **48**: 1–9.
- Klionsky DJ, Abdalla FC, Abeliovich H, et al. Guidelines for the use and interpretation of assays for monitoring autophagy. *Autophagy* 2012; **8**: 445–544.
- Sakai T, Kamiya T, Oikawa M, Sato T, Tanaka A, Ishii K. JAERI Takasaki in-air micro-PIXE system for various applications. *Nucl Instrum Methods Phys Res B* 2002; **190**: 271–275.
- Kozai N, Mitamura H, Ohnuki T, Sakai T, Sato T, Oikawa M. Application of micro-PIXE to quantitative analysis of heavy elements sorbed on minerals. *Nucl Instrum Methods Phys Res B* 2005; **231**: 530–535.
- Shimizu Y, Dobashi K. Proton ion-microbeam elemental analysis for inhaled particle-induced pulmonary diseases: application for diagnosis and assessment of progression. *Curr Med Chem* 2013; **20**: 789–793.
- Ohta K, Nakano J, Nishizawa M, et al. Suppressive effect of antisense DNA of platelet-derived growth factor on murine pulmonary fibrosis with silica particles. *Chest* 1997; **111**(6 Suppl): 105S.
- Shimizu Y, Dobashi K, Kusakbe T, et al. In-air micro-particle induced X-ray emission analysis of asbestos and metals in lung tissue. *Int J Immunopathol Pharmacol* 2008; **21**: 567–576.
- Matsuzaki S, Shimizu Y, Dobashi K, et al. Analysis on the co-localization of asbestos bodies and Fas or CD163 expression in asbestos lung tissue by in-air micro-pixe. *Int J Immunopathol Pharmacol* 2010; **23**: 1–11.
- Bara M, Moretto P, Razafindrabe L, Llabador Y, Simonoff M, Guet-Bara A. Nuclear microanalysis of the effect of magnesium and taurine on the ionic distribution in the human amniotic membrane. *Cell Mol Biol (Noisy-le-grand)* 1996; **42**: 27–38.
- Shimizu Y, Matsuzaki S, Dobashi K, et al. Elemental analysis of lung tissue particles and intracellular iron content of alveolar macrophages in pulmonary alveolar proteinosis. *Respir Res* 2011; **12**: 88.
- Borges VM, Lopes MF, Falcão H, et al. Apoptosis underlies immunopathogenic mechanisms in acute silicosis. *Am J Respir Cell Mol Biol* 2002;

- 27: 78–84.
- 41 Yao SQ, Rojanasakul LW, Chen ZY, *et al.* Fas/FasL pathway-mediated alveolar macrophage apoptosis involved in human silicosis. *Apoptosis* 2011; **12**: 1195–1204.
 - 42 Kajiwara T, Ogami A, Yamato H, Oyabu T, Morimoto Y, Tanaka I. Effect of particle size of intratracheally instilled crystalline silica on pulmonary inflammation. *J Occup Health* 2007; **49**: 88–94.
 - 43 Bjørkøy G, Lamark T, Brech A, *et al.* p62/SQSTM1 forms protein aggregates degraded by autophagy and has a protective effect on huntingtin-induced cell death. *J Cell Biol* 2005; **171**: 603–614.
 - 44 Young SL, Crapo JD, Kremers SA, Brumley GW. Pulmonary surfactant lipid production in oxygen-exposed rat lungs. *Lab Invest* 1982; **46**: 570–576.
 - 45 Pascolo L, Gianoncelli A, Schneider G, *et al.* The interaction of asbestos and iron in lung tissue revealed by synchrotron-based scanning X-ray microscopy. *Sci Rep* 2013; **3**: 1123.
 - 46 Ghio AJ, Tong H, Soukup JM, *et al.* Sequestration of mitochondrial iron by silica particle initiates a biological effect. *Am J Physiol Lung Cell Mol Physiol* 2013; **305**: L712–L724.
 - 47 Patel AS, Lin L, Geyer A, *et al.* Autophagy in idiopathic pulmonary fibrosis. *PLoS One* 2012; **7**: e41394.
 - 48 Monick MM, Powers LS, Walters K, *et al.* Identification of an autophagy defect in smokers' alveolar macrophages. *J Immunol* 2010; **185**: 5425–5435.
 - 49 Araya J, Kojima J, Takasaka N, *et al.* Insufficient autophagy in idiopathic pulmonary fibrosis. *Am J Physiol Lung Cell Mol Physiol* 2013; **304**: L56–L69.
 - 50 Moscat J, Diaz-Meco MT. p62: a versatile multitasker takes on cancer. *Trends Biochem Sci* 2012; **37**: 230–236.
 - 51 Young MM, Takahashi Y, Khan O, *et al.* Autophagosomal membrane serves as platform for intracellular death-inducing signaling complex (iDISC)-mediated caspase-8 activation and apoptosis. *J Biol Chem* 2012; **287**: 12455–12468.
 - 52 Liang X, Wei SQ, Lee SJ, *et al.* p62 sequestosome 1/light chain 3b complex confers cytoprotection on lung epithelial cells after hyperoxia. *Am J Respir Cell Mol Biol* 2013; **48**: 489–496.
 - 53 Ahmed Z, Tabrizi SJ, Li A, *et al.* A Huntington's disease phenocopy characterized by pallido-nigro-luysian degeneration with brain iron accumulation and p62-positive glial inclusions. *Neuropathol Appl Neurobiol* 2010; **36**: 551–557.
 - 54 Khan MI, Mohammad A, Patil G, Naqvi SA, Chauhan LK, Ahmad I. Induction of ROS, mitochondrial damage and autophagy in lung epithelial cancer cells by iron oxide nanoparticles. *Biomaterials* 2012; **33**: 1477–1488.
 - 55 Sun T, Yan Y, Zhao Y, Guo F, Jiang C. Copper oxide nanoparticles induce autophagic cell death in A549 cells. *PLoS One* 2012; **7**: e43442.
 - 56 Refsnes M, Hetland RB, Øvrevik J, Sundfjør I, Schwarze PE, Låg M. Different particle determinants induce apoptosis and cytokine release in primary alveolar macrophage cultures. *Part Fibre Toxicol* 2006; **3**: 10.
 - 57 Nagatomo H, Morimoto Y, Oyabu T, *et al.* Expression of heme oxygenase-1 in the lungs of rats exposed to crystalline silica. *J Occup Health* 2006; **48**: 124–128.